Interaction of Oleic Acid with Dipalmitoylphosphatidylcholine (DPPC) Bilayers Simulated by Molecular Dynamics

ARTICLE *in* THE JOURNAL OF PHYSICAL CHEMISTRY B · DECEMBER 2007

Impact Factor: 3.3 · DOI: 10.1021/jp0723564 · Source: PubMed

3 AUTHORS, INCLUDING:

Rebecca Notman
The University of Warwick
23 PUBLICATIONS **432** CITATIONS
SEE PROFILE

Jamshed Anwar
Lancaster University
74 PUBLICATIONS **1,589** CITATIONS
SEE PROFILE

Interaction of Oleic Acid with Dipalmitoylphosphatidylcholine (DPPC) Bilayers Simulated by Molecular Dynamics

Rebecca Notman,[†] Massimo G. Noro,[‡] and Jamshed Anwar*[,§]

Molecular Biophysics, Division of Pharmaceutical Science, King's College London, Franklin-Wilkins Building, Stamford Street, London, SE1 9NH U.K., Physical and Chemical Insight Group, Unilever Research & Development Port Sunlight, Wirral, CH63 3JW U.K., and Computational Laboratory, Institute of Pharmaceutical Innovation, University of Bradford, Bradford, West Yorkshire, BD1 7DP U.K.

Received: March 25, 2007; In Final Form: August 20, 2007

The fatty acid oleic acid (OA) is known to modulate the structure of membranes, which forms the basis for a number of its important applications including its use as a therapeutic supplement to reduce the risk of cardiovascular disease, in molecule delivery systems such as liposomes, and as a skin permeability enhancer. While a number of studies have investigated the effect of OA on lipid membranes, our understanding of its mechanisms of action at the molecular level remains rudimentary. We have carried out molecular dynamics simulations using coarse-grained models to investigate the interactions of OA at a range of concentrations with a dipalmitoylphosphatidylcholine (DPPC) bilayer in the liquid-crystalline phase. We have also investigated the relative permeability of the bilayers to model hydrophilic and hydrophobic penetrants by means of chemical potential calculations. The results indicate that OA is able to disperse homogeneously into the bilayer at all concentrations without much perturbation. OA appears to slightly weaken the lateral forces between lipid headgroups, and as the concentration of OA increases this manifests itself as a slight decrease in the area compressibility modulus and a minor increase in the diffusion rate of the OA molecules. While the chemical potential profiles showed little or no variation as a function of OA concentration, the frequency of water permeation events was found to double, indicating some OA-induced permeability enhancement. The study suggests that physiological effects of OA are probably more subtle rather than via gross perturbation of the structure, or that its significant effects are restricted to more condensed membrane structures such as the gel phase.

Introduction

Oleic acid (*cis*-octadec-9-enoic acid, $CH_3(CH_2)_7HC{=}CH(CH_2)_7COOH$) is one of the most abundant fatty acids in nature. It is of significant therapeutic value and has important technological applications that include its use in molecule delivery systems such as liposomes. In terms of its therapeutic activity, oleic acid (OA) is a prototype in a paradigm shift in therapeutics where the focus is on modulating the lipid composition and microstructure of membranes (membrane−lipid therapy),[1] rather than the classical approach of directly rectifying malfunctions in the activity of nucleic acids and proteins. OA is known to reduce the risk of cardiovascular disease (by regulating G-protein function via its action on the lipid structure) and cancer,[2] and it has been associated with loss of body weight. In terms of applications, it is used at low concentrations as a surfactant in inhalers that deliver actives into the lung and as an adjuvant in liposomes where it is considered to improve the delivery of encapsulated agents, possibly by increasing the flexibility of the liposomes.[3] OA is also an effective penetration enhancer that increases the permeability of the lipid layers of the stratum corneum (the outermost layer of the skin) to facilitate the delivery of active molecules topically to the skin or transdermally.[4−7]

While the effect of OA on phospholipids has been investigated in numerous studies,[2,3,8−10] our molecular level understanding of its interaction with the phospholipids is still rudimentary. With regard to its effect on the phase behavior of phospholipid membranes, OA has been found to slightly decrease the gel-to-liquid crystalline phase transition temperature of dipalmitoylphosphatidylcholine (DPPC) bilayers from 41 to 37°C at concentrations up to ∼33 mole % OA,[3,8] which suggests some degree of fluidization of the bilayer by OA. Experiments on DPPC monolayers have shown that OA has a minor condensing effect resulting from the attenuation of the repulsion between the charged headgroups (oleic acid is uncharged), but at the same time it also disturbs the packing of the of acyl chains.[11] When incorporated into DPPC liposomes, OA causes an increase in the flux of the encapsulated (biologically active) molecule, which is thought to be due to an increase in the fluidity and associated enhanced flexibility of the liposomes.[3] These effects tend to be in contrast to those of *trans*-unsaturated or -saturated fatty acids, for example, stearic acid, which tend to make the bilayer more rigid.[8] Consequently, molecular shape is perceived to be important, as the major difference between these molecules and OA is the presence of the *cis*-unsaturated bond in OA that causes it to adopt a "kinked" conformation. It is intuitive to suggest that the presence of this kink disrupts the packing of the phospholipids in an ordered bilayer. There is also some evidence that phase separation of OA and DPPC occurs in DPPC monolayers at high surface pressures, in DPPC liposomes,[9] and in the DPPC gel phase[8] at high concentrations

* Author to whom correspondence should be addressed. Tel.: +44 1274 236145. E-mail:j.anwar@bradford.ac.uk.
[†] King's College London.
[‡] Unilever Research & Development Port Sunlight.
[§] University of Bradford.

10.1021/jp0723564 CCC: $37.00
Published on Web 10/16/2007

of OA. However, it is unclear whether this phase separation occurs in DPPC bilayers in the fluid bilayer phase.

The interaction of OA with the lipids of the stratum corneum and how it enhances the penetration of a variety of polar and nonpolar molecules through the skin is also not well understood. The lipid layers of the stratum corneum contain virtually no phospholipids; instead they are comprised mainly of ceramides, cholesterol, and free fatty acids. As with phospholipid bilayers, OA lowers the gel-to-liquid crystalline phase transition temperature of the stratum corneum,[5,6,12] and this has been directly correlated to an increase in permeation.[13] Again, it is thought that OA disrupts the packing of the stratum corneum lipids because of its "kinked" structure, making it easier for third-party molecules to diffuse through. It has also been shown that at physiological temperatures, that is, below the transition temperature, OA exists as a separate phase within the stratum corneum. These considerations suggest a number of possible mechanisms and associated pathways by which OA may facilitate the transport of penetrant molecules. Possibilities include fluidization of the bilayer making it easier for a penetrant to permeate, OA-induced inter-digitation with associated reduction in bilayer thickness and a reduced path length, and/or a lower barrier pathway at interfacial defects that may arise around OA molecules within the bilayer.[13,14] In addition, should phase separation occur, the penetrant molecules may diffuse directly through the liquid OA phase. The mechanisms of action of OA are likely to be different in the skin from that in phospholipid membranes because of the nature of the lipids and their phase behavior.

We report here the interaction of OA with DPPC in the fluid phase with a particular focus on its effect on the bilayer permeability as observed by molecular dynamics (MD) simulations. The simulations employ coarse-grained models where a group of several atoms is represented by a single interaction center.[15,16] These coarse-grained simulations enable longer length and time-scale phenomena to be accessed at the expense of some atomic detail. As the effects of oleic acid may be concentration-dependent, we have investigated a range of concentrations of oleic acid in the bilayer. The permeability of the bilayer membranes was characterized for both polar and nonpolar penetrants by means of chemical potential calculations.

Methods

The MD simulations were carried out on a system comprising 512 DPPC molecules in the liquid-crystalline phase containing varying concentrations of OA in the protonated form. The pK_a of OA is about 7.5,[17] but the bilayer experiments and liposomal applications span a pH range from about 5 to 7 at which the protonated form dominates. For this reason we opted for the protonated form. A study that investigated the effect of ionization of the fatty acid dodecanoic acid on the properties of 1,2-dilauroyl-*sn*-glycerol monolayers containing dodecanoic acid suggests that the effects of ionization of OA on the system are likely to be marginal.[18] The OA concentrations investigated were 0 (pure DPPC), 0.05, 0.1, 0.2, 0.4, 0.6, 0.8, and 1 (pure OA) mole fraction with respect to the lipid. The simulations were carried out in an NPT ensemble with anisotropic (orthogonal) pressure coupling at 323 K and 1 bar using the GROMACS molecular simulation package version 3.2.[19] The molecular interaction cutoffs for both the van der Waals and the electrostatics were 1.2 nm. The time step employed was 40 fs. Such large timesteps become feasible as a consequence of the coarse graining of the modeled systems.

We used a coarse-grained (CG) model in which a group of atoms is represented by a single interaction site. The CG force field employed has been developed to reproduce the structural, elastic, and dynamic properties of a range of phospholipids.[15] In this force field, the CG particles interact via a Lennard-Jones potential and the electrostatics are truncated. The model of OA was built from the available particle types within the CG force field and consisted of a single polar headgroup particle bonded to a chain of five lipid tail particles. Out of the two possible choices for the headgroup particle (polar particle type P or nonpolar particle with hydrogen-bond donor and acceptor groups Nad), the polar particle type P was chosen being deemed to be the best representation of the mainly polar carboxyl group of OA. A weak harmonic potential ($k_{bond} = 1250$ kJ mol^{-1} nm^{-2}) kept the bonded particles together, while a cosine angle potential with a force constant k_{ang} of 25 kJ mol^{-1} rad^{-2} was used to maintain chain stiffness. The "*cis*-unsaturated bond" in the hydrocarbon chain of the OA molecule was introduced using a cosine potential with a force constant $k_{ang} = 35$ kJ mol^{-1} rad^{-2} and an equilibrium angle of 120°. These force constant and equilibrium angle values were taken from the CG force field[16] which has also been parametrized for unsaturated hydrocarbon chains.

TABLE 1: Compositions of the Systems Simulated in the Study

[OA] (mole fraction)	number of CG lipid molecules or water particles[a] DPPC	OA	water
0.0	512	0	5888
0.05	486	26	5739
0.1	461	51	5595
0.2	410	102	5302
0.4	307	205	4709
0.6	205	307	4123
0.8	102	410	3531
1.0	0	512	2944

[a] Note that one CG water particle is equivalent to four real water molecules.

The starting configurations for the simulations were generated by replicating a single DPPC molecule along the *x*- and *y*-directions to create a monolayer and then replicating and inverting the monolayer to create a bilayer with the normal parallel to the *z*-direction. Water molecules were added to maintain a ratio of 46 water molecules per lipid (23 water molecules per lipid tail). The DPPC system was equilibrated for 30 ns, and the OA molecules were inserted into the bilayer by replacing some of the DPPC molecules randomly with OA to achieve the desired concentration. For each concentration the system was further equilibrated for 10 ns. For the systems containing OA, the number of water molecules was adjusted to maintain a constant concentration of 23 water molecules per lipid tail (i.e., 23 water molecules per OA). The compositions of the various systems studied are given in Table 1. The production simulations were run for 800 ns. Although the bilayers appeared to equilibrate fairly rapidly (for example, the area per lipid converged within 100 ns), only the final 400 ns trajectory was used for analysis. This was to ensure more complete mixing of the OA with DPPC, in case the effects of insufficient mixing were too subtle to have an effect on the parameters used to determine equilibration.

To characterize the permeability of the DPPC/OA bilayers, we used Widom's particle insertion technique[20] to calculate the chemical potential of model polar and nonpolar CG particles as a function of distance along the bilayer normal. A more common approach is to carry out a potential of mean force (PMF) calculation for the penetrant molecule.[21] This approach

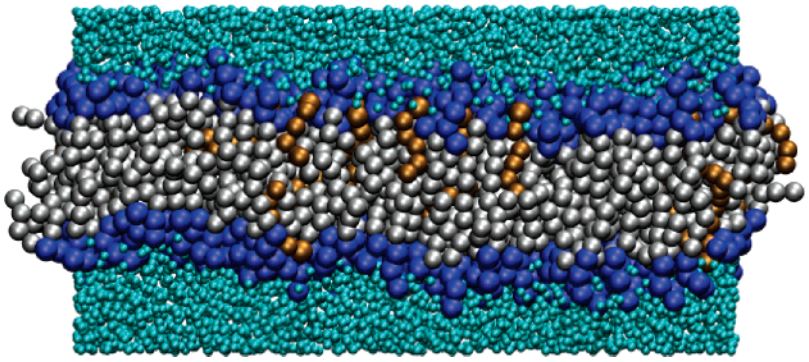

Figure 1. Snapshot of the DPPC bilayer containing 0.2 mole fraction OA. Water is shown in cyan, DPPC headgroups and glycerol backbone particles in blue, DPPC tails in light gray, and OA molecules in brown. The image was generated using VMD.[27]

is rather tedious, requiring a whole series of simulations with the penetrant molecules being either constrained or restrained (umbrella sampling) at various points on the reaction coordinate. Such PMF calculations were not considered appropriate as our intention was get a relative indication of the free energy barrier, and the particle insertion approach yields the required data and offers considerable efficiency. The particle insertion chemical potential calculations do not require specific simulations with the penetrant molecules being present in the system: the calculations can be carried out post-simulation on the main trajectories. In the particle insertion method, the excess chemical potential μ_{ex} of a particle in the NPT ensemble is given by

$$\mu_{ex} = -k_B T \ln[\langle V \rangle^{-1} \langle V \exp(-U_{N+1}/k_B T) \rangle]$$

where k_B is the Boltzmann constant, N the number of particles in the system, T the absolute temperature, V the volume of the simulation cell, and U_{N+1} is the energy of the interaction between the randomly inserted $N+1$ particle (the penetrant molecule) and the rest of the system. To produce the chemical potential profile across the bilayer, we divided the simulation box into 10 slices perpendicular to the bilayer normal. By determining which slice the inserted particle is in, μ_{ex} can be averaged for each slice. An issue arises with this method for high-density systems where U_{N+1} is often too high to contribute to the average in the above equation, making the estimate of μ_{ex} unreliable.[22] To overcome this in our high-density system (the reduced density $\rho = 0.85$) we reduced the σ-parameter of the LJ interaction of our model molecules, a hydrophilic and a hydrophobic CG particle, to 0.8σ, hence reducing the effective diameter of the particles. The 0.8σ value was chosen as test calculations revealed that this was the largest effective particle size that enabled the particle insertion calculations to converge within a reasonable number of insertions (5×10^7 insertions over 160 ns of trajectory).

Results and Discussion

In general, OA at all concentrations had very little effect on the overall structure of the bilayer. The nature of OA enabled it to integrate well into the existing bilayer structure both in the hydrocarbon region and at the interface. A snapshot from the simulation trajectory for the DPPC bilayer with 0.2 mole fraction OA is shown in Figure 1. The trajectories show that the OA molecules interact with the hydrocarbon chains of the DPPC molecules and disperse homogeneously throughout the bilayer. The density profiles of the membrane components, computed by dividing the simulation box into slices perpendicular to the bilayer normal, for the DPPC bilayer containing 0.2 mole fraction OA are shown in Figure 2. OA appears to sit

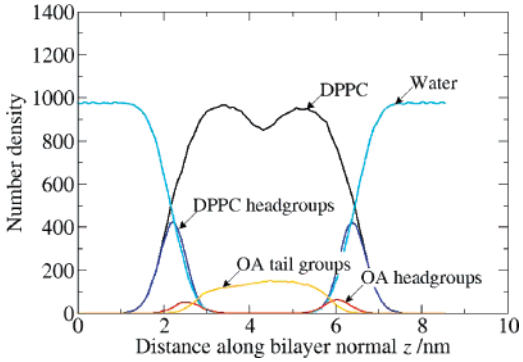

Figure 2. Density profiles of the various components and moieties comprising the DPPC bilayer with 0.2 mole fraction OA.

with its polar particle located below the phosphate group of the lipids and its hydrocarbon chain within the hydrocarbon region of the bilayer. This position of OA in the bilayer corresponds exactly to that tentatively proposed by El Maghraby et al.[3] In this position, OA in principle could disrupt both the packing of the DPPC at the polar/nonpolar interface and in the hydrocarbon region.

No phase separation was observed at any of the concentrations of OA investigated. These observations, at first, seem at odds with experimental findings that OA and DPPC undergo phase separation at high concentrations of OA.[8,9,14] However, our findings should perhaps not be so surprising as the DPPC bilayer in the simulations is in the liquid-crystalline phase and phase separation of OA with phospholipids has been observed only in the gel phase and at lower temperatures (or high surface pressures in monolayer experiments). In addition, DSC experiments have suggested that DPPC and OA may form a number of undefined liquid phases at temperatures greater than ~313 K and at oleic acid concentrations greater than 0.75 mole fraction.[8] The simulations even at high concentrations of OA did not show any noticeable heterogeneity in the DPPC/OA systems that might be indicative of some preferred complexation between DPPC and OA. We infer that the liquid-crystalline phase DPPC bilayer is sufficiently fluid to accommodate the "kink" in the OA hydrocarbon chain without much energetic cost and hence enables OA to disperse homogenously within it.

The amount of "free volume" in a membrane, that is, the space not occupied by lipids or water, is determined by the molecular packing of the lipids and can influence membrane properties such as lateral diffusion, compressibility modulus, and permeability.[23] An additive molecule such as OA may alter the extent of free volume in different regions of the bilayer. To explore the effects of OA we computed both the projected area

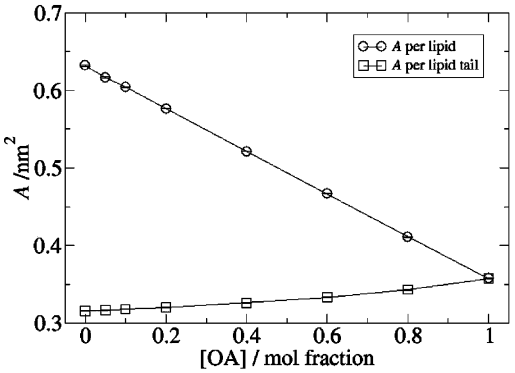

Figure 3. Area per lipid (OA and DPPC molecules) and area per lipid tail as a function of the concentration of OA in the bilayer. The error bars refer to standard deviations that were estimated by block averaging.

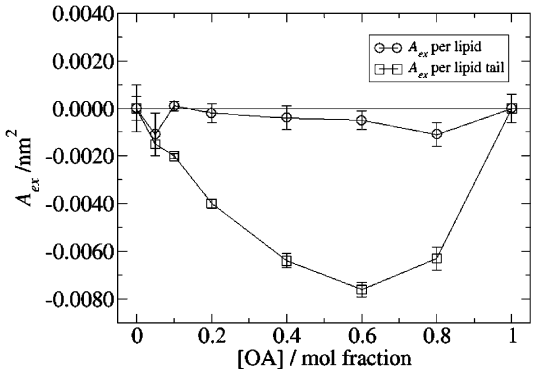

Figure 4. Thermodynamic excess area A_{ex} per lipid and per lipid tail as a function of the mole fraction of OA in the DPPC/OA bilayer.

per lipid (the lipid definition in this instance includes both OA and DPPC) and the area per tail. Both quantities are shown plotted in Figure 3 as a function of the OA concentration. The area per molecule decreases linearly with increasing OA concentration which indicates that the effect of OA on the headgroup region of the bilayer is purely additive and that OA does not modulate the packing in this region. In contrast, the area per tail shows a slight negative deviation from linearity, suggesting a slight reduction in the "free area" in this region. A more meaningful quantity is the thermodynamic excess area A_{ex}, which is the difference between the actual area per lipid (or lipid tail) in the mixture and the ideal area per lipid (or lipid tail) calculated from the pure bilayers, as a function of the mole fraction of OA in the bilayer. The thermodynamic excess areas, area per lipid and area per tail, are shown in Figure 4. The excess area per lipid shows very little variation from zero, while the excess area per tail shows a minor reduction indicating some condensation of the bilayers. These results are in good agreement with surface pressure−area experiments on Langmuir films of mixed DPPC/OA monolayers which show little or no deviation from ideal mixing behavior of DPPC and OA,[10] or a slight negative deviation from ideal indicating minor condensation of the bilayer induced by OA.[11]

The bilayer thickness, obtained from the distance between the peaks of the phosphate density distribution, for each system as a function of the OA concentration is shown in Figure 5. There is essentially no variation in the bilayer thickness with an increase in the OA concentration, other than the pure OA system being ~0.5 nm thinner than the DPPC/OA bilayers. This suggests that there is neither OA-induced interdigitation nor increased fluidization of the bilayer. The latter effect would reduce the bilayer thickness, as the increased disorder in the alkyl chains results in a reduction in their effective lengths. The

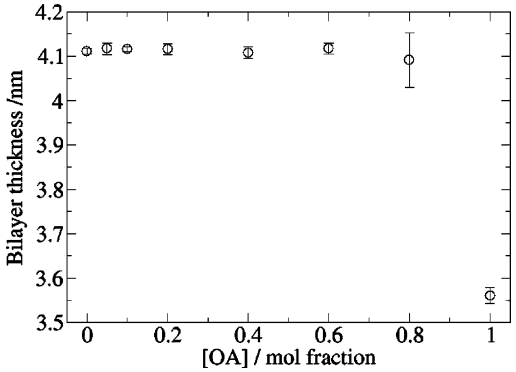

Figure 5. Thickness of the bilayer with increasing OA concentration. The error bars show the standard deviations that were estimated by block averaging.

slightly lower bilayer thickness of the pure OA bilayer is accounted for by the fact that although OA has 5 tail particles compared to 4 for DPPC, OA lacks the bulky headgroup of DPPC. On the basis of little or no variation in bilayer thickness, we expect that the lipid chain ordering is unaffected by OA. To verify this, we looked at the effect of OA on the alignment of the lipid tails with respect to the bilayer normal by calculating lipid tail order parameters: $S_z = {}^3/_2\langle\cos^2\theta_z\rangle - {}^1/_2$ where, for a carbon atom C_n, θ_z is the angle between the vector C_{n-1} to C_{n+1} and the *z*-axis of the simulation box. Order parameters were computed for consecutive lipid tail particles and averaged over both tails. In a completely ordered chain $S_z = 1$; for an entirely random orientation $S_z = 0$. The order parameters (Figure 6) reveal that there is no change in the disorder of the lipid tails at OA concentrations up to 0.2 mole fraction. Above this concentration there is a marginal increase in the disorder of the lipid tails with increasing OA concentration. It is interesting to note that we observe a slight increase in disorder of the lipid tails while the excess area per tail data indicates minor condensation of the bilayer, this point having been noted earlier in a mixed DPPC/OA monolayer study.[10] These apparently contrasting effects, however, are rather marginal and do not warrant any in-depth discussion. It would be useful to compare the computed lipid order parameters with order parameters obtained from neutron-scattering experiments, but to our knowledge these experiments have not yet been carried out.

As the polar carboxyl group of OA sits just below the water/bilayer interface, it is reasonable to propose that OA may affect membrane permeability by disrupting this interfacial region. To determine the effect of OA on the interface, we calculated the bilayer/water interfacial width, which is defined as the distance over which the water density falls from 90 to 10% of its bulk value. Figure 7 shows that the interfacial width shows only a slight change with increasing OA concentration, which indicates that OA is readily incorporated into the bilayer and does not disrupt the packing at the interface. The interface is actually narrower for the pure OA bilayer than for the DPPC/OA bilayers, probably because OA has a smaller headgroup than DPPC.

The bilayer thickness and order parameter results suggest that the fluidity of the lipid chains is only marginally changed in the presence of OA. However, the bilayer may also be fluidized with respect to the mobility of the lipids in the plane of the bilayer. The lateral diffusion coefficients of the DPPC and OA molecules, calculated from the gradient of the mean squared displacement plots for the period 400−800 ns, as a function of OA concentration are plotted in Figure 8. It is immediately apparent that the OA has a greater lateral mobility than the

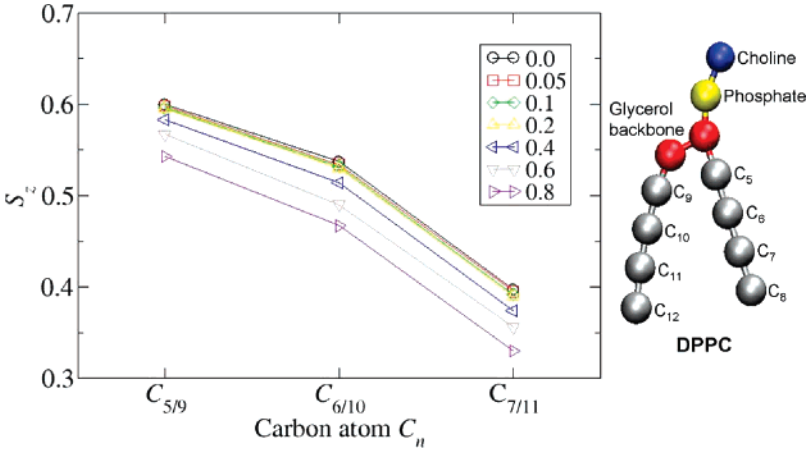

Figure 6. Order parameters for the DPPC tail particles, averaged over both tails. The numbering of the DPPC carbon atoms corresponds to the image on the right. Estimated standard error was ±0.02.

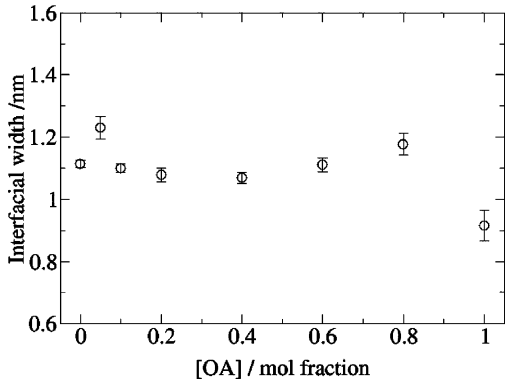

Figure 7. Width of the water/bilayer interface at different concentrations of OA. The error bars refer to standard deviations that were estimated by block averaging.

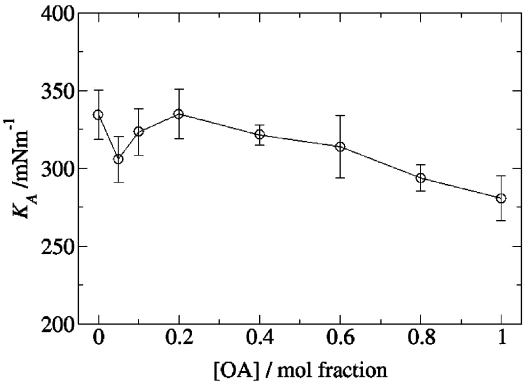

Figure 9. Area compressibility K_A of the DPPC/OA bilayers as a function of OA concentration in the bilayer calculated from simulations at constant area per lipid. Errors were estimated from the fit of the surface tension as a function of area per lipid.

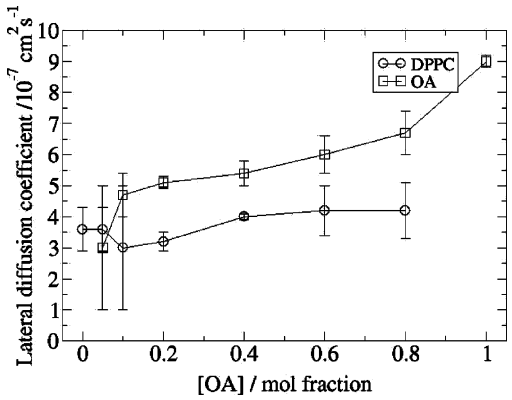

Figure 8. Lateral diffusion coefficients calculated from mean squared displacements of the DPPC molecules (circles) and OA molecules (squares) as a function of OA concentration.

phospholipids. This is in agreement with the results of fluorescence quenching experiments where the lateral diffusion coefficient of a probe molecule was a factor of 2 larger in OA monolayers than in phospholipid monolayers.[24] The lateral diffusion of DPPC remains essentially unchanged with an increase in OA concentration, while the lateral diffusion of the incorporated OA shows a slight increase with increase in OA concentration. It seems that OA may be exerting some cooperative effect in enhancing its own rate of diffusion as its concentration increases.

The effect of OA on the rigidity of the bilayer was investigated using the method of Feller and Pastor[25] where the area compressibility modulus for each bilayer is calculated from a series of simulations at fixed area per lipid. The area compressibility moduli K_A as a function of the OA concentration in the bilayer are shown in Figure 9. While at low concentrations of OA there is little change in K_A, at higher concentrations from upward of 0.2 mole fraction there is a gradual decrease in K_A indicating that as OA is increased the bilayer becomes more compressible, requiring lower energy to either stretch or compress it. The implication is that individual lipid molecules are less constrained by the surrounding matrix of molecules. The enhanced OA-induced flexibility of the bilayers is consistent with the experimental observations that OA causes DPPC liposomes to become more flexible.[3]

To characterize the permeability of the DPPC/OA bilayers, we calculated the excess chemical potential of a model hydrophilic and a model hydrophobic particle across the bilayer. Although the calculation of the permeability coefficient also requires knowledge of the diffusion rate of the penetrant molecule as a function of position across the bilayer, the permeability coefficient is dominated by the chemical potential profile. The chemical potential profiles for the hydrophobic and hydrophilic penetrant particles in the various DPPC/OA systems including the pure OA system are given in Figures 10 and 11, respectively. For the hydrophobic particle, the highest point of the chemical potential profile corresponds to the solvent-phase region and the solvent− headgroup interface, indicating these regions as the location of the main barrier to penetration. The chemical potential decreases considerably in going toward the center of the bilayer (but for a very minor peak in the center, the origin of which is discussed below), which clearly identifies

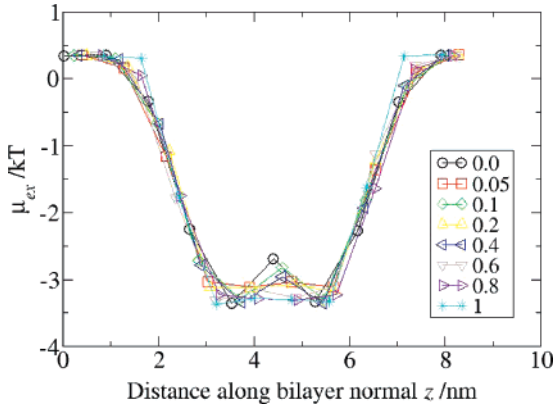

Figure 10. Excess chemical potential profiles of a hydrophobic particle across a DPPC bilayer containing different concentrations of OA.

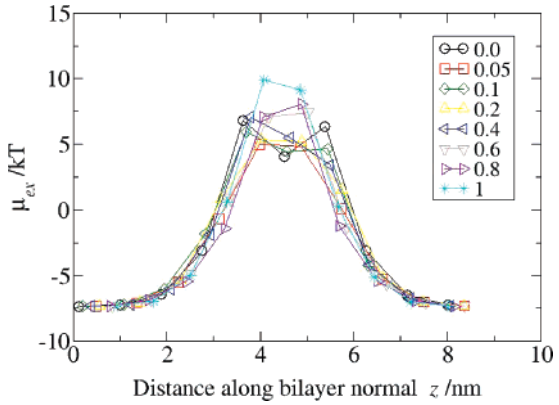

Figure 11. Chemical potential profiles of a hydrophilic particle across a DPPC bilayer containing different concentrations of OA.

the affinity of the hydrophobic particle for the hydrocarbon region of the bilayer. The chemical potential profiles are pretty much superposed, indicating that OA does not appear to influence the penetration of hydrophobic particles in these systems. The pure OA bilayer has a marginally steeper chemical potential profile than those of the mixed systems. This is probably because the interfacial width of the pure OA bilayers is much narrower (see Figure 7), which results from OA having a much smaller headgroup than DPPC. A more defined, smaller headgroup limits the distribution of the solvent particles, making the change of environment from hydrophilic to hydrophobic much sharper. For the hydrophilic particle (Figure 11), the chemical potential profiles are inverted and peak in the central region of the bilayer but for a minor trough for some of the systems at the bilayer center. The profiles confirm that the barrier to penetration for hydrophilic particles lies in the central region of the bilayer. Once more, the chemical potential profiles show hardly any variation as the concentration of OA is increased, suggesting that OA does not significantly alter the permeability of the DPPC bilayers to hydrophilic particles. The height of the barrier for the pure OA bilayer is slightly higher than that for the mixed DPPC/OA systems. This suggests that if phase separation and pooling of OA were to take place, the OA pools presenting a high barrier do not offer an advantageous alternative pathway relative to DPPC bilayers. Comparing the chemical potential profiles for the hydrophobic and hydrophilic particles, it is apparent that the barrier to penetration of hydrophilic particles ($\sim 18kT$) is significantly greater than that of hydrophobic particles ($\sim 4kT$), probably because the bilayer is predominantly a hydrophobic environment. As noted above, the chemical potential profiles reveal a minor peak for the hydrophobic particle and a minor trough for the hydrophilic

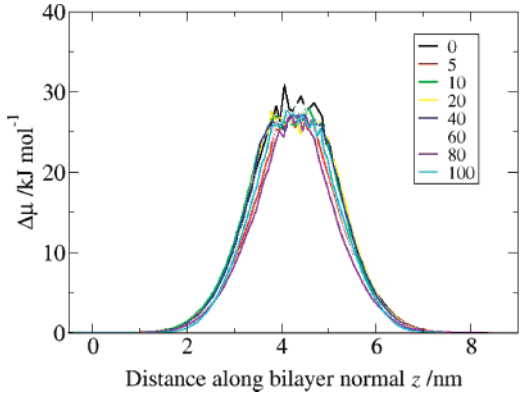

Figure 12. Chemical potential profile for a water particle as a function of the distance along the bilayer normal. The chemical potential difference is with respect to that in the water region.

particle at the center of the bilayer for the pure DPPC systems, which become insignificant with an increase in OA concentration. We believe that the minor peak and trough are linked and are probably a consequence of the lipid tails having a lower density in the center of the bilayer. For the hydrophilic particle, the minor trough reflects the increased free volume at the bilayer center. For the hydrophobic particle, the minor peak (an increase in chemical potential) probably results from the greater affinity of the hydrophobic penetrant for the hydrophobic tail particles (this interaction is actually attractive) than for free space.

Recounting that the chemical potential profiles refer to test particles whose characteristic length scale, the LJ σ-parameter, has been scaled by a factor of 0.8, it would be beneficial to extrapolate or correlate these profiles to what might be expected for full-sized CG particles. To our knowledge, there is no simple or ready extrapolation procedure or relationship to enable this. It is, however, possible to correlate the profiles of the hydrophilic particle to a true CG particle with polar characteristics, namely, a water particle, since water permeation events are observed in the simulations. Although these permeation events are rather limited (typically 3 to 6 particle crossings in 100 ns), a chemical potential profile of the water particle can be estimated from $\Delta\mu(z) = k_B T \ln(\rho_{eq}/\rho_z)$, where ρ_{eq} is the average density of the particle in bulk water and $\rho(z)$ is the average density of the particle as a function of its position along the membrane normal. As calculated, the estimated chemical potential difference is with respect to that in the water region. The estimated chemical potential profiles of the water particle for the various bilayers containing increasing amounts of OA are shown in Figure 12. While the chemical potential profiles do not show much discrimination as a function of OA concentration, the minor differences do manifest in the permeation events. For the pure DPPC bilayer patch of 512 lipids, we obtained three permeation events for the water particle per 100 ns, which is slightly higher than the rate of one event per 100 ns for a patch of 256 lipids as reported by Marrink for the same model.[15] The permeation rate increases by a factor of 2 to ~6 CG particles per 100 ns for all of the bilayers containing OA, including the pure OA bilayer. This indicates that the flux of water through the bilayer does, in fact, increase upon the addition of OA.

We note that many of the results of the system containing 0.05 mole fraction OA tend to be slightly out of line with respect to other OA concentrations. The bilayer lipids appear to have some additional freedom which results in a slightly higher diffusion constant of DPPC and a larger interfacial width (presumably as the solvent can penetrate a little more deeply into the bilayer), and we also see a slightly lower compressibility modulus compared with adjacent systems with either higher or

lower levels of OA. We are currently at a loss as to what might be the underlying cause.

Reviewing the results, OA at all concentrations appears to integrate without much perturbation into the DPPC bilayer with the OA−DPPC interaction being essentially ideal. There is only a marginal decrease in the thermodynamic excess area, and no phase separation was observed. The OA-induced variation in bilayer thickness was found to be minimal, and there was only a marginal increase in the disorder of the lipid tails. The interfacial width showed a slight increase with increasing OA concentration. With respect to mechanical properties, there was a small reduction in the compressibility modulus of the bilayers. The chemical potential profiles that characterize the permeability of the bilayer systems were found not to be much affected by OA for the hydrophobic and hydrophilic probe particles. Despite the lack of discrimination between the chemical potential profiles, we do however note a small increase in permeability of the bilayers to water in the presence of OA. On the whole, these findings contrast with the expectation that the kink in the oleic acid hydrocarbon chain should result in a looser packing of the bilayer molecules. It seems as if the flexibility of the DPPC hydrocarbon chains is sufficient in accommodating the OA kinked molecule. While these results on the fluid phase of DPPC may be contrary to expectations (mostly because the expectations are linked to the bilayer being in the gel phase), they do not contradict any of the experimental observations. OA does appear to have a minor penetration enhancement role in the fluid DPPC bilayers, but this cannot be attributed to any single particular effect, the two main contributors probably being the enhanced compressibility and the slight decrease in the tail disorder. The simulations also dispel, to some extent, the notion that phase separation of OA might be an important element in the mechanism of action of OA in enhancing penetration in the fluid DPPC phase: there is no phase separation and, even if it did occur, the OA pool does not represent an easier pathway relative to the DPPC bilayer. The role of phase separation, however, cannot be ruled out for gel-phase structures where the OA−DPPC interface could present a lower barrier to penetration. Finally, we note that the reduction in the effective lipid−lipid interaction induced by OA that gives rise to an enhancement in the compressibility of the fluid DPPC layer could have a more marked effect for the gel phase. This would be consistent with experimental observations of oleic acid inducing greater flexibility of liposomes, the effect of which is to facilitate the release of active molecules from these vesicles. Clearly, simulations investigating the effects of OA on DPPC bilayers in the gel phase would be invaluable but are outside of the scope of the present study. Gel-phase simulations, particularly of heterogeneous multicomponent systems that may phase separate, can present major technical challenges because of ergodicity problems. The dynamics of such systems are relatively slow, with any ''equilibrated'' structure being, in general, not too dissimilar to the starting configuration.

We acknowledge that the results need some qualifications that arise from the coarse-grained models employed. The coarse-grained models enable access to long time scales, which is a particularly important requirement for the problem studied, as the system needs sufficient time to deal with lipid mixing and the possibility of phase separation of the OA and DDPC components. On the whole, the CG models employed are respectable: the DPPC model is well characterized and the parameters of the OA model can be readily mapped as the molecule does not differ much from molecular types validated by the CG forcefield. Probably the critical feature is the *cis*-unsaturated bond which is implemented by a bond-angle potential. The magnitude of the force constant for this potential could bias the results. Indeed,we note that in the recently published revision of CG forcefield, MARTINI[26] (that came to our attention after submission of this manuscript), this force constant has been increased from 35 to 45 kJ mol^{-1}. A slightly more rigid angle is likely to make the OA a little more disruptive, possibly further increasing tail disorder and, in turn, the permeability of the bilayer.

Conclusions

The molecular dynamics simulations reveal that OA at all concentrations is able to integrate and homogenously disperse within liquid crystalline DPPC bilayers without inducing much perturbation. OA is able to induce an increase in permeability of water and reduces the compressibility modulus of the bilayer, but both effects are small. The study suggests that physiological effects of OA are probably more subtle rather than via gross perturbation of the structure, or that its significant effects are restricted to more condensed membrane structures such as the gel phase.

Acknowledgment. R.N. is grateful to the EPSRC and Unilever Research for the provision of an industrial CASE studentship.

References and Notes

(1) Escriba, P. V. Membrane-lipid therapy: A new approach in molecular medicine. *Trends Mol. Med.* **2006**, *12* (1), 34−43.

(2) Funari, S. S.; Barcelo, F.; Escriba, P. V. Effects of oleic acid and its congeners, elaidic and stearic acids, on the structural properties of phosphatidylethanolamine membranes. *J. Lipid Res.* **2003**, *44*, 567−575.

(3) el Maghraby, G. M. M.; Williams, A. C.; Barry, B. W. Interactions of surfactants (edge activators) and skin penetration enhancers with liposomes. *Int. J. Pharm.* **2004**, *276* (1−2), 143−161.

(4) Cooper, E. R. Increased skin permeability for lipophilic molecules. *J. Pharm. Sci.* **1984**, *73* (8), 1153−1156.

(5) Barry, B. W. Mode of action of penetration enhancers in human skin. *J. Controlled Release* **1987**, *6* (1), 85−97.

(6) Barry, B. W.; Bennett, S. L. Effect of penetration enhancers on the permeation of mannitol, hyrocortisone, and progesterone through human skin. *J. Pharm. Pharmacol.* **1987**, *39* (7), 535−546.

(7) Golden, G. M.; McKie, J. E.; Potts, R. O. Role of stratum corneum lipid fluidity in transdermal drug flux. *J. Pharm. Sci.* **1987**, *76* (1), 25−28.

(8) Inoue, T.; Yanagihara, S.; Misono, Y.; Suzuki, M. Effect of fatty acids on phase behaviour of hydrated dipalmitoylphosphatidylcholine bilayer: Saturated versus unsaturated fatty acids. *Chem. Phys. Lipids* **2001**, *109* (2), 117−133.

(9) Busquets, M. A.; Mestres, C.; Alsina, M. A.; Anton, J. M. G.; Reig, F. Miscibility of dipalmitoylphosphatidylcholine, oleic acid, and cholesterol measured by DSC and compression isotherms of monolayers. *Thermochim. Acta* **1994**, *232* (2), 261−269.

(10) Lewis, D.; Hadgraft, J. Mixed monolayers of dipalmitoylphosphatidylcholine with azone or oleic acid at the air−water interface. *Int. J. Pharm.* **1990**, *65* (3), 211−218.

(11) Gonçalves da Silva, A. M.; Romão, R. I. Mixed monolayers involving DPPC, DODAB, and oleic acid and their interaction with nicotinic acid at the air−water interface. *Chem. Phys. Lipids* **2005**, *137* (1−2), 62−76.

(12) Tanojo, H.; BosvanGeest, A.; Bouwstra, J. A.; Junginger, H. E.; Bodde, H. E. In vitro human skin barrier perturbation by oleic acid: Thermal analysis and freeze fracture electron microscopy studies. *Thermochim. Acta* **1997**, *293* (1−2), 77−85.

(13) Francoeur, M. L.; Golden, G. M.; Potts, R. O. Oleic acid: Its effects on stratum corneum in relation to (trans)dermal drug delivery. *Pharm. Res.* **1990**, *7* (6), 621−627.

(14) Ongpipattanakul, B.; Burnette, R. R.; Potts, R. O.; Francoeur, M. L. Evidence that oleic acid exists in a separate phase within stratum corneum lipids. *Pharm. Res.* **1991**, *8* (3), 350−354.

(15) Marrink, S. J.; de Vries, A. H.; Mark, A. E. Coarse-grained model for semiquantitative lipid simulations. *J. Phys. Chem. B* **2004**, *108* (2), 750−760.

(16) Shelley, J. C.; Shelley, M. Y.; Reeder, R. C.; Bandyopadhyay, S.; Klein, M. L. A coarse-grain model for phospholipid simulations. *J. Phys. Chem. B* **2001**, *105* (19), 4464−4470.

(17) Hamilton, J. A.; Cistola, D. P. Transfer of oleic acid between albumin and phospholipid vesicles. *Proc. Natl. Acad. Sci. U.S.A.* **1986**, *83*, 82−86.

(18) van Buuren, A. R.; Tieleman, D. P.; de Vlieg, J.; Berendsen, H. J. C. Cosurfactants lower surface tension of the diaglyceride/water interface: A molecular dynamics study. *Langmuir* **1996**, *12*, 2570−2579.

(19) Lindahl, E.; Hess, B.; van der Spoel, D. GROMACS 3.0: A package for molecular simulation and trajectory analysis. *J. Mol. Model.* **2001**, *7* (8), 306−317.

(20) Widom, B. Some topics in the theory of fluids. *J. Chem. Phys.* **1963**, *39* (11), 2802−2812.

(21) Marrink, S. J.; Berendsen, H. J. C. Simulation of water transport through a lipid membrane. *J. Phys. Chem.* **1994**, *98* (15), 4155−4168.

(22) Frenkel, D.; Smit, B., *Understanding molecular simulation: From algorithms to applications*. Academic Press: San Diego, 1996.

(23) Falck, E.; Patra, M.; Karttunen, M.; Hyvonen, M. T.; Vattulainen, I. Lessons of slicing membranes: Interplay of packing, free area, and lateral diffusion in phospholipid/cholesterol bilayers. *Biophys. J.* **2004**, *87* (2), 1076−1091.

(24) Caruso, F.; Grieser, F.; Thistlethwaite, P. J. Lateral diffusion of amphiphiles in fatty acid monolayers at the air−water interface: A steady-state and time-resolved fluorescence quenching study. *Langmuir* **1993**, *9* (11), 3142−3148.

(25) Feller, S. E.; Pastor, R. W. Constant surface tension simulations of lipid bilayers: The sensitivity of surface areas and compressibilities. *J. Chem. Phys.* **1999**, *111* (3), 1281−1287.

(26) Marrink, S. J.; Risselada, H. J.; Yefimov, S.; Tieleman, D. P.; de Vries, A. H. The MARTINI force field: Coarse-grained model for biomolecular simulations. *J. Phys. Chem. B* **2007**, *111* (27), 7812−7824.

(27) Humphrey, W.; Dalke, A.; Schulten, K. VMD: Visual molecular dynamics. *J. Mol. Graphics* **1996**, *14* (1), 33−38.